Available online at www.sciencedirect.com
SCIENCE DIRECT®
ELSEVIER
Earth and Planetary Science Letters 220 (2004) 409–421
EPSL
www.elsevier.com/locate/epsl

A 90° spin on Rodinia: possible causal links between the Neoproterozoic supercontinent, superplume, true polar wander and low-latitude glaciation☆

Z.X. Li[a,*], D.A.D. Evans[a,b], S. Zhang[c]

[a] Tectonics Special Research Centre, The University of Western Australia, Crawley, WA 6009, Australia
[b] Department of Geology and Geophysics, Yale University, P.O. Box 208109, New Haven, CT 06520, USA
[c] School of Earth and Land Resources, China University of Geosciences, Beijing 10083, PR China

Received 5 September 2003; received in revised form 20 January 2004; accepted 21 January 2004

Abstract

We report here new geochronological and paleomagnetic data from the 802 ± 10 Ma Xiaofeng dykes in South China. Together with existing data, these results suggest that Rodinia probably spread from the equator to the polar region at ca. 800 Ma, followed by a rapid ca. 90° rotation around an axis near Greenland that brought the entire supercontinent to a low-latitude position by ca. 750 Ma. We propose that it was the initiation of a mantle superplume under the polar end of Rodinia that triggered an episode of true polar wander (TPW) which brought the entire supercontinent into equatorial latitudes. An unusually extensive emerged land area at the equator increased both atmospheric CO_2 drawdown and global albedo, which, along with waning plume volcanism led directly to the low-latitude Sturtian glaciation at ca. 750–720 Ma.

Keywords: Rodinia; supercontinent; Neoproterozoic; paleomagnetism; South China; superplume; true polar wander

1. Introduction

Fragmentation of the early Neoproterozoic supercontinent Rodinia [1–3] coincided with a remarkable series of geological events. Widespread non-orogenic, bimodal magmatism between 830 and 740 Ma, accompanied by lithospheric doming and continental rifting, has been interpreted as indicating the existence of a mantle superplume under Rodinia that eventually disaggregated the supercontinent [4]. Near-equatorial glacial deposits at this time at sea level [5] have led to the hypothesis of one or more snowball Earth episodes [6,7]. Is there any causal relationship between these events? In this paper we present geochronological and paleomagnetic results from the Xiaofeng dykes in South China that together with similar-aged results from other continents, can best be interpreted as indicating a ca. 90° true polar wander (TPW) event between ca. 800 and 750 Ma. This enables us to explore possible genet-

* Corresponding author. Fax: +61-8-6488-1037.
E-mail address: zli@tsrc.uwa.edu.au (Z.X. Li).

☆ Supplementary data associated with this article can be found at S0012821X04000640

0012-821X/04/$ – see front matter © 2004 Elsevier B.V. All rights reserved.
doi:10.1016/S0012-821X(04)00064-0

ic linkages between the formation and breakup of the supercontinent Rodinia, the Rodinian superplume, the TPW event, and the ca. 750–720 Ma low-latitude glaciation.

2. Regional geology and SHRIMP U–Pb zircon age determination

The Xiaofeng dykes are a chemically composite suite (SiO_2 contents between 47 and 76%) intruding the 819 ± 7 Ma Huangling Batholith [8,9] in the Three Gorges region of the South China Block (Fig. 1a). The dykes are sub-vertical, with strikes varying between 37 and ca. 70°, and thicknesses between a few centimeters and over 20 m. The densest occurrence of the dykes is found along the southeastern margin of the Huangling Batholith just north of Xiaofeng, where dykes account for 65–80% of the rock volume in a zone of up to 3 km wide (Fig. 1) [9]. Locally porphyritic, felsic dykes are seen to be cross-cut by thinner, more mafic dykes; however, all the dykes are regarded as being of the same generation [9] because (1) the chemical compositions of the Xiaofeng dykes are composite between the more mafic and felsic endmembers, (2) there is no difference in either orientation or spatial distribution between dykes of different compositions, and (3) all dykes intrude the Huangling Batholith and are non-conformably overlain by the 748 ± 12 Ma [10] Liantuo Formation, a non-metamor-

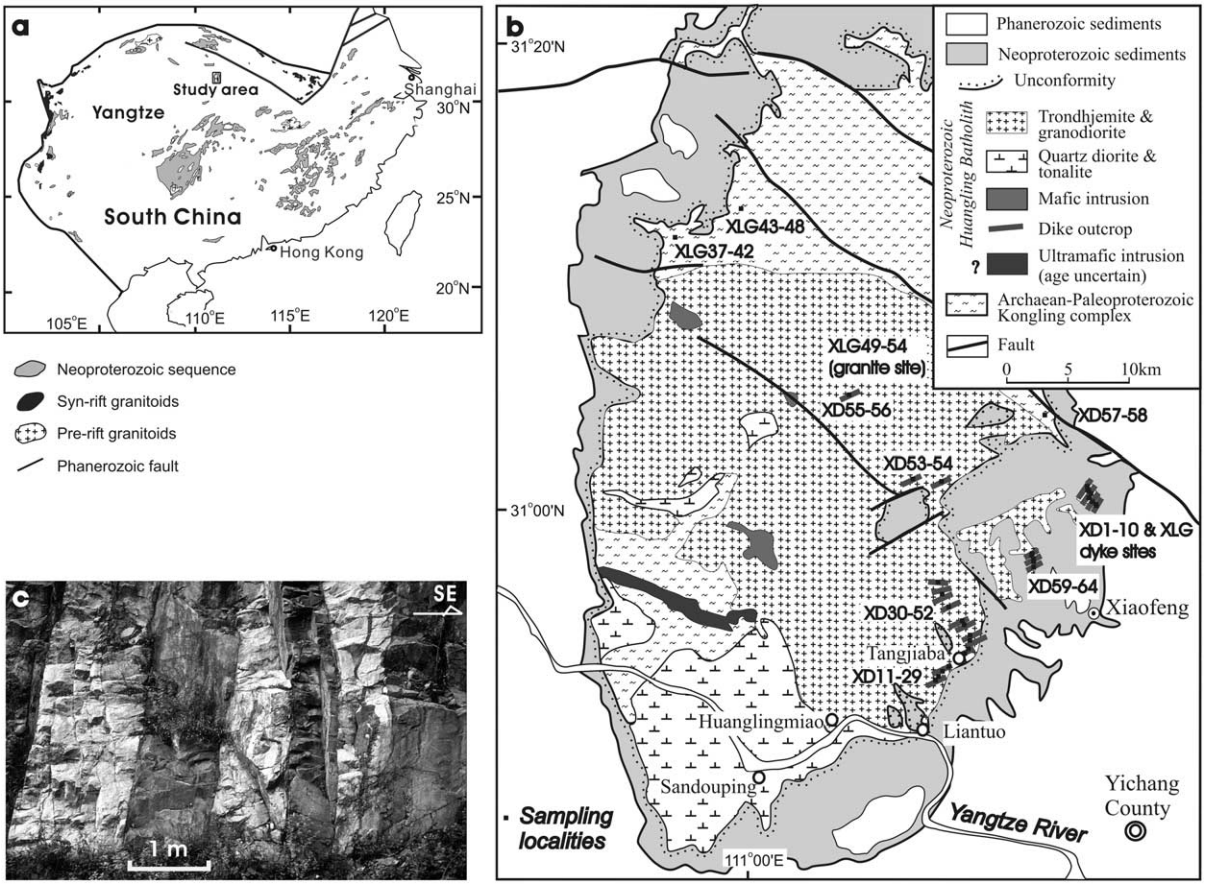

Fig. 1. Localities of paleomagnetic sampling (a, b) and a photo showing the 802 ± 10 Ma mafic dykes (dark colored) intruding the 819 ± 7 Ma Huangling granitoid (light colored) (c).

phosed siliciclastic unit with a gentle dip of ca. 10° toward the southeast throughout the study region. The age of the Xiaofeng dykes is thus constrained to be between 819 ± 7 and 748 ± 12 Ma.

To obtain a more precise age constraint on the Xiaofeng dykes, we collected two block samples for age determinations: one from an intermediate dyke, and another from a pale-gray colored, porphyritic felsic member of the dykes (SiO_2 = 65.2%). Whereas the intermediate sample failed to produce zircon grains suitable for SHRIMP dating, the more felsic sample (99SC01; location 31°00.868′N, 111°17.569′E, which is between paleomagnetic sites HLG7–12 and HLG13–18) yielded sufficient quantity of euhedral magmatic zircon grains of 70–300 μm dimension.

Twenty grains from the latter sample were analyzed on the SHRIMP-II ion microprobe at Curtin University of Technology following standard procedures [11]. The measured isotopic ratios and calculated ages for individual spot analyses are given in Table 1, and concordia plots of results in Fig. 2. Of the 20 grains analyzed, grains 6 and 11 are discordant, and grain 17 gives a significantly younger (ca. 750 Ma) age than the bulk of the analyses. These three grains likely have suffered Pb loss. Grains 8 and 9 are also excluded from mean-age calculation because their $^{206}Pb/^{238}U$ ages are more than two standard deviations away from the mean value, likely due to xenocrystic inheritance. The remaining 15 analyses give a weighted mean $^{206}Pb/^{238}U$ age of 802 ± 10 Ma (2σ; MSWD = 1.02), taken as the crystallization age of the dykes.

3. Paleomagnetic results

We collected 450 oriented samples from 77 sites for paleomagnetic analyses, including 72 sites from the dykes (commonly one site per dyke, mainly mafic dykes sampled), and five sites from the country rocks (Fig. 1). The country rocks away from the dense dyke swarm (both the 819 ± 7 Ma Huangling Batholith and the Archaean–Paleoproterozoic Kongling Complex) were sampled in order to perform a baked contact test [12]. At all sites, one specimen from each sample was subjected to stepwise thermal demagnetization, and some selected specimens subjected

Table 1
SHRIMP zircon U–Pb data from sample 99SC1[a]

Spot	U (ppm)	Th (ppm)	Th/U	%com ^{206}Pb	$^{207}Pb/^{206}Pb$	±1σ	$^{206}Pb/^{238}U$	±1σ	$^{207}Pb/^{235}U$	±1σ	Age $^{206}Pb/^{238}U$	±1σ
8	155	232	1.49	0.61%	0.0659	0.0020	0.1410	0.0022	1.281	0.046	850	12
9	98	125	1.27	1.29%	0.0656	0.0028	0.1379	0.0022	1.247	0.060	833	13
14	152	165	1.08	0.33%	0.0667	0.0016	0.1363	0.0020	1.254	0.038	824	12
15	164	186	1.13	0.81%	0.0642	0.0019	0.1360	0.0020	1.204	0.041	822	12
18	125	145	1.16	0.58%	0.0671	0.0027	0.1342	0.0021	1.242	0.057	812	12
4	415	509	1.23	0.54%	0.0677	0.0011	0.1341	0.0018	1.252	0.028	811	10
1	114	186	1.63	2.45%	0.0701	0.0037	0.1334	0.0021	1.289	0.074	807	12
20	193	200	1.04	0.18%	0.0676	0.0016	0.1327	0.0019	1.237	0.036	803	11
13	72	109	1.52	0.97%	0.0697	0.0039	0.1322	0.0023	1.271	0.078	801	13
5	322	672	2.09	0.92%	0.0652	0.0014	0.1320	0.0018	1.187	0.033	799	11
19	154	356	2.31	1.16%	0.0632	0.0023	0.1320	0.0020	1.149	0.047	799	11
16	199	287	1.44	0.11%	0.0685	0.0013	0.1316	0.0019	1.244	0.032	797	11
7	116	188	1.61	0.35%	0.0693	0.0024	0.1315	0.0021	1.256	0.050	796	12
3	213	351	1.65	0.67%	0.0660	0.0016	0.1310	0.0019	1.193	0.036	794	11
12	173	192	1.11	0.34%	0.0684	0.0019	0.1309	0.0019	1.235	0.040	793	11
10	65	73	1.13	0.72%	0.0684	0.0042	0.1299	0.0023	1.224	0.080	787	13
2	307	537	1.75	0.29%	0.0674	0.0011	0.1289	0.0018	1.197	0.027	782	10
17	139	390	2.81	3.96%	0.0647	0.0044	0.1226	0.0020	1.094	0.079	746	11
11	195	234	1.20	1.59%	0.0703	0.0034	0.1062	0.0016	1.029	0.053	651	9
6	369	641	1.74	4.95%	0.0665	0.0030	0.1048	0.0015	0.961	0.047	642	9

[a] Radiogenic lead corrected using ^{204}Pb.

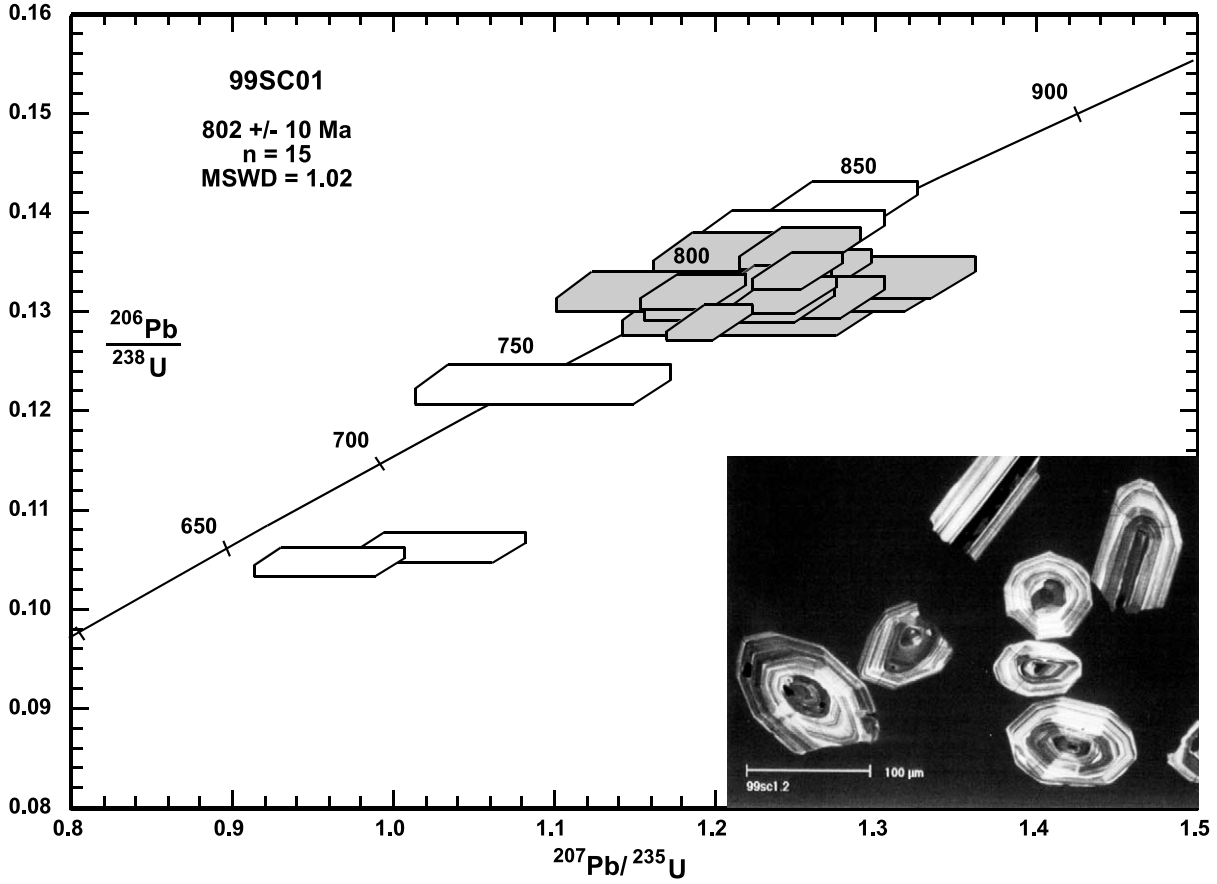

Fig. 2. Concordia plots of SHRIMP U–Pb zircon analyses and cathodoluminescence (CL) images of some of the zircon crystals. Analyses used for calculating the mean age are shown in gray.

to alternating-field demagnetization, with remanent magnetization measured on a 2G-755 cryogenic magnetometer in the University of Western Australia.

Principal component analysis [13] revealed two consistent remanence vectors from the dykes. The first one is a low- to intermediate-temperature component (C1) that conforms to the Present geomagnetic dipole field direction (Fig. 3a,c–e; Table 2[1]). This component is present in almost all the sites investigated.

The second component (C2) is a high-temperature steep two-polarity characteristic remanence. It is found in 168 samples from 54 sites (Fig. 3; Table 3). The remanence typically has unblocking temperatures between 500 and 580°C, approaching the Curie temperature of magnetite (Fig. 3a–d). This, together with the susceptibility–temperature curves (Fig. 3c–d), suggests that C2 is likely carried by pseudo-single-domain magnetite. Whereas C2 from the majority of the dykes gives steep-negative inclinations, on four occasions we observed steep-positive inclinations (Fig. 3b; Table 3). The in situ mean direction of C2 is: $D = 087.6°$, $I = -72.3°$, $N = 54$, $\alpha_{95} = 6.1°$ and $k = 11.1$. After the gentle dip corrections restoring the overlying Neoproterozoic succession to horizontal, the mean direction becomes $D = 051.3°$, $I = -76.6°$, $N = 54$, $\alpha_{95} = 6.1°$ and $k = 11.2$.

Although we sampled both the Archaean–Paleoproterozoic Kongling Complex (sites XD57,

[1] See online version of this article.

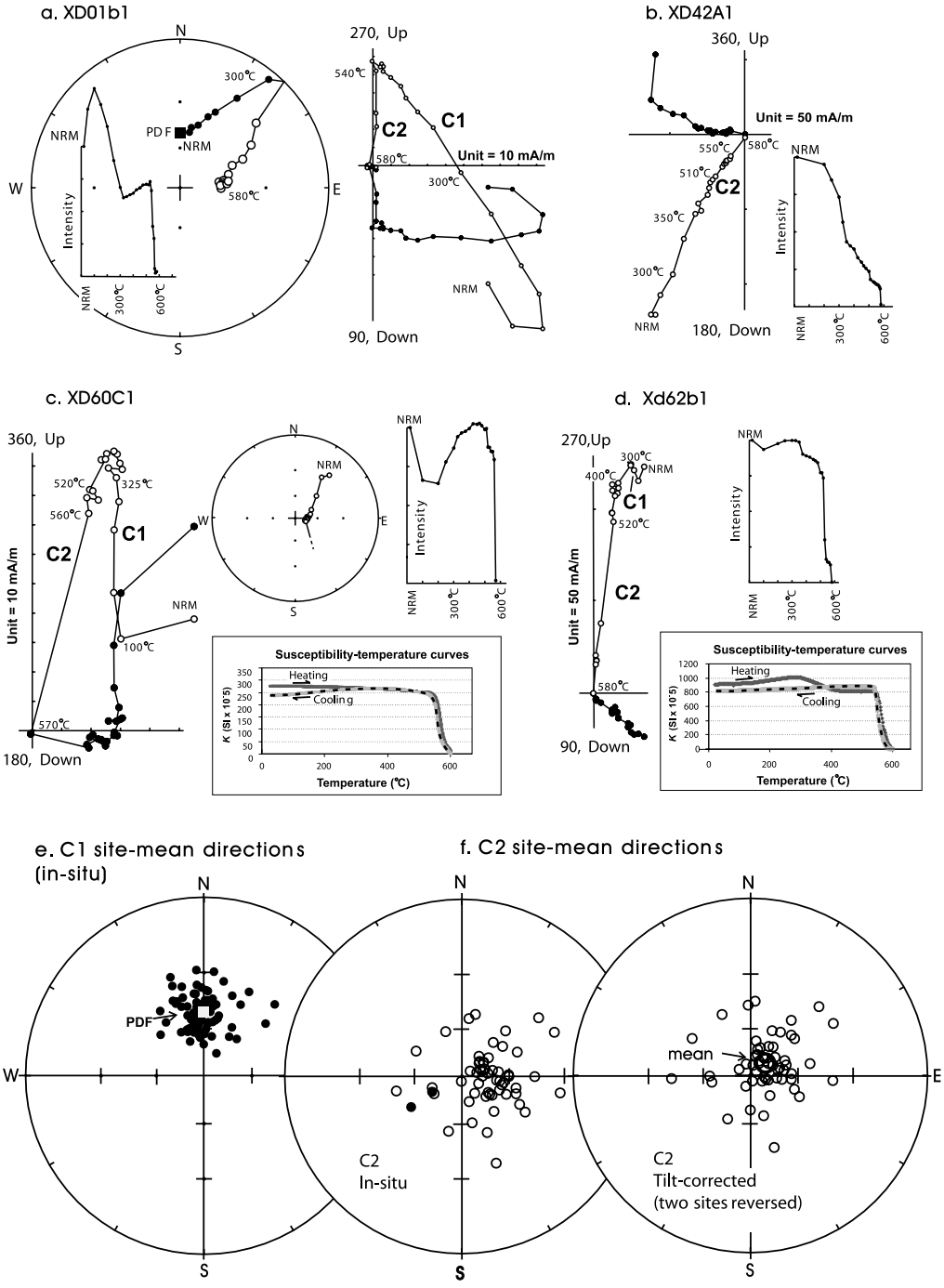

Fig. 3. Representative demagnetization data (a–d), in situ site mean direction of the viscous component C1 (e), and site mean directions of the characteristic remanence component C2 (f). For the orthogonal plots, open (closed) circles are projections on the vertical (horizontal) planes. The stereographic plots are in equal-angle projections, where open (closed) circles are projections on the upper (lower) hemisphere. Results of two magnetic susceptibility–temperature measurements, using a Bartington MS2 W/F system, are shown in inserts of (c) and (d).

Table 3
Site mean directions of the characteristic remanence (C2) from the Xiaofeng dykes

Site	In situ		Tectonic corrected		n/n_o	α_{95}	Tectonic correction	
	Dec. (°)	Inc. (°)	Dec. (°)	Inc. (°)		(°)	R-hand strike	Dip
XD01	89.9	−60.3	73.7	−66.2	6/6	5.7	46	10
XD02	109.8	−64.6	95.6	−73.0	3/7	20.8	46	10
XD03	249.3	−69.7	269.1	−64.1	1/7	–	46	10
XD04	12.3	−50.6	3.7	−44.4	6/6	12.2	46	10
XD06	49.5	−75.1	15.3	−72.6	7/9	14.9	46	10
XD09	42.7	−60.7	25.9	−58.6	4/6	24.9	46	10
XD10A	299.0	−57.1	302.4	−47.5	2/3	–	46	10
XD10B	238.9	53.0	225.4	54.1	4/4	32.2	46	10
XD11	53.6	−58.1	34.7	−56.9	2/6	–	50	12
XD12	107.7	−54.4	95.1	−63.8	1/7	–	50	12
XD14	99.5	−31.3	93.5	−40.0	4/4	13.1	50	12
XD17	111.9	−59.8	97.0	−69.7	2/5	–	50	12
XD18	83.1	−73.2	9.6	−75.7	5/6	2.7	50	12
XD19	155.7	−51.7	161.7	−63.1	2/5	–	50	12
XD21	82.8	−66.5	53.5	−70.4	2/5	–	50	12
XD22	96.0	−67.7	65.8	−74.1	1/6	–	50	12
XD23	57.7	−73.6	19.9	−71.1	5/5	16.3	50	12
XD24	90.1	−45.3	78.8	−52.1	2/6	–	50	12
XD25	87.9	−60.5	66.5	−66.1	2/5	–	50	12
XD28	40.2	−73.0	9.3	−67.7	3/4	22.5	50	12
XD32	340.1	−59.9	335.1	−48.4	4/6	25.7	50	12
XD33	89.1	−76.7	31.3	−79.1	1/5	–	50	12
XD34	257.5	−48.5	267.7	−42.0	5/5	5.2	50	12
XD36	115.8	−50.2	107.5	−60.8	4/6	13.7	50	12
XD38	129.8	−70.0	115.7	−81.5	2/6	–	50	12
XD39	163.9	−73.2	203.1	−82.5	3/6	12.9	50	12
XD41	122.5	−68.9	102.7	−79.7	4/6	8.5	50	12
XD42[a]	121.9	−67.3	104.3	−78.1	5/5	13.3	50	12
XD43[a]	121.2	−70.3	97.0	−80.8	3/5	20.0	50	12
XD44	101.8	−64.1	78.8	−72.0	3/7	13.4	50	12
XD45	102.0	−55.3	87.4	−63.8	5/6	9.8	50	12
XD46[a]	242.8	68.6	212.2	68.1	5/6	11.7	50	12
XD47	98.4	−63.3	75.7	−70.7	3/5	10.6	50	12
XD48	66.2	−52.3	50.2	−54.0	4/6	4.5	50	12
XD49	52.6	−32.8	44.9	−32.5	4/6	11.4	50	12
XD50	119.4	−45.4	113.5	−56.4	1/6	–	50	12
XD52	137.4	−60.0	135.8	−72.0	5/6	12.6	50	12
XD53	54.8	−69.2	38.5	−66.7	6/6	5.2	67	7
XD54	96.6	−65.7	81.2	−68.3	3/7	31.8	67	7
XD56	43.8	−50.8	36.5	−47.6	1/6	–	67	7
XD58	63.7	−29.6	57.9	−32.2	3/6	22.5	46	10
XD59	56.8	−73.3	25.0	−75.7	7/7	5.0	26	9
XD60	51.9	−75.9	14.0	−77.1	6/6	11.0	26	9
XD61	74.8	−80.0	13.7	−83.3	6/6	7.8	26	9
XD62	57.1	−83.6	340.1	−82.1	5/5	4.4	26	9
XD63	74.2	−76.0	35.3	−80.6	3/4	3.2	26	9
XD64	78.8	−70.0	56.6	−76.1	5/6	18.8	26	9
HLG13–18	185.6	−86.8	298.8	−81.7	5/6	11.1	46	10
HLG19–24	142.6	−76.4	159.8	−86.2	4/6	20.2	46	10
HLG25–30	112.7	−78.3	55.5	−85.3	3/6	4.4	46	10
HLG31–36	38.2	−69.1	260.1	−65.1	4/6	18.5	46	10

Table 3 (*Continued*).

Site	In situ		Tectonic corrected		n/n_o	α_{95}	Tectonic correction	
	Dec. (°)	Inc. (°)	Dec. (°)	Inc. (°)		(°)	R-hand strike	Dip
HLG60–64	67.5	−60.0	180.1	−68.0	1/5	–	46	10
HLG65–69	6.9	−53.6	358.2	−46.7	3/5	2.7	46	10
HLG75–80	93.7	−54.7	207.6	−59.0	6/6	8.2	46	10
Mean directions:								
	87.6	−72.3	51.3	−76.6	$N=54$			
	$\alpha_{95}=6.1$	$k=11.1$	$\alpha_{95}=6.1$	$k=11.2$				
			Pole position from tectonic-corrected direction, using site location (30.96°N, 111.23°E): (13.5°N, 91.0°E), dp = 10.5°, dm = 11.3°					

For most of the results, each site represents an individual dyke.
n = number of samples accepted form each site; n_o = total number of samples analyzed.
[a] Sites with mixed polarities. Sites XD42 and XD43 both contain samples from small mafic veins close to, but not necessarily part of, the main dykes sampled; Site XD46 is 4 m away from a group of closely-spaced dykes (sites XD45 and XD47) that gave the opposite remanent direction.

XD58, XLG37–42 and XLG43–48) and the 819 ± 7 Ma Huangling Batholith (sites XLG49–54) for a baked contact test, unfortunately none of those sites revealed well-defined remanence vectors apart from a viscous component from sites XD57 and XD58. We interpret component C2 as a primary remanence representative of the time-averaged Neoproterozoic geomagnetic field based on the following observations: (1) the overlying little-deformed Liantuo Formation retains a primary magnetization [14,15], indicating that there has been no pervasive overprint event in the region; (2) the remanence direction is dissimilar to any known younger magnetizations expected of the region, including that from the overlying ca. 750 Ma Liantuo Formation; (3) the unblocking temperatures are commonly between 500 and 580°C (Fig. 3), typical of low-titanium magnetite of magmatic origin; (4) there is no evidence of the region being heated to elevated temperatures since the intrusion of the dykes; and (5) the presence of dual polarity and moderate standard deviation about the mean indicate adequate time averaging of geomagnetic secular variation.

The gentle dipping of the overlying strata and the sub-vertical nature of the dykes indicate that the region has not been tilted significantly since ca. 750 Ma, and we are thus able to provide a good control on the paleohorizontal of the dykes. The fact that there is no systematic difference between dykes of different chemical compositions reinforces the geological interpretation that the studied dykes belong to the same generation [9]. The paleomagnetic pole from the tilt-corrected mean C2 direction is located at 13.5°N, 091.0°E, with dp = 10.5°, dm = 11.3°. We interpret the SHRIMP result of 802 ± 10 Ma as the age of this paleopole.

4. Geodynamic interpretations

4.1. Rodinia reconstructions, and a possible TPW event

Our new paleomagnetic pole places South China at 55–70° paleolatitude at ca. 800 Ma, in par with high paleolatitude indicated by a similarly-aged pole from India. However, presumed coeval paleomagnetic data from Laurentia and Australia [16] indicate low-latitude positions that would appear to separate these cratons substantially from the high-latitude continents. We consider three possible interpretations for these results. One is that an equatorial Rodinia supercontinent excluded high-latitude cratons such as South China and India [17]. However, such a paleogeography has difficulty in explaining striking similarities

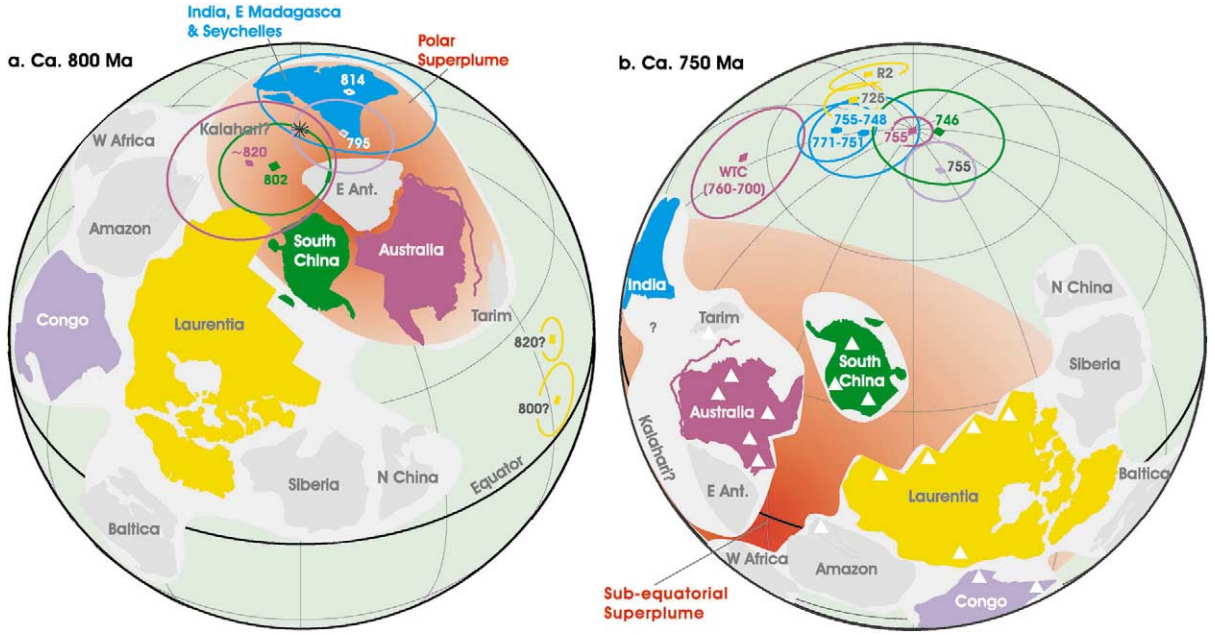

Fig. 4. Paleogeographic reconstructions of Rodinia (a) at ca. 800 Ma and (b) during its breakup at ca. 750 Ma according to one possible scenario, in which South China was located between Australia and Laurentia, and Rodinia broke apart by ca. 750 Ma. Paleopoles are color-coded to their host cratons with numbers showing their ages in Ma. South China poles (green): 802 ± 10 Ma Xiaofeng dykes (this study), and 748 ± 12 Ma Liantuo pole [14,15]; Indian (blue) poles: 814 ± 34 Ma Harohalli dykes pole [19], the 771–751 Ma Malani Igneous Suite pole [54], and the rotated pole from the 755–748 Ma Mahe dykes from Seychelles [55]; Australia (violet): the ca. 820 Ma Wooltana Volcanics pole [20], the WTC pole from the cap dolomite of the Walsh Tillite (putative Sturtian equivalent) [56], and the 755 ± 3 Ma Mundine Well dykes pole [25]; Congo (indigo): 795 ± 7 Ma Gagwe lavas pole [21,22], and the 755 ± 25 Ma Mbozi Complex pole [21]; Laurentia (yellow): R2 pole from the Rapitan glacial deposits [26], and others from the compilation of McElhinny and McFadden [12]. Note that the age and reliability of 820–800 Ma Laurentian poles are highly uncertain [24]. Key Euler poles used in (a) are: Congo (43.0, 029.1, 92.4), Laurentia (41.5, −168.0, 115.1), South China (−26.7, −030.9, 85.1), Australia (−10.6, −013.9, 156.3), India (20.5, 167.3, −78.3). Sources of relative positions for other continents, where no paleomagnetic constraint is available for the times concerned, are: Baltica [24], Siberia [57], North China and Tarim [58]. The position of the Amazon craton relative to Laurentia is slightly readjusted from the position suggested by Tohver et al. [59]. White triangles in (b) show the occurrence of the Sturtian glacial deposits.

in Neoproterozoic magmatic and rifting events among India, South China, Australia and Laurentia [4,18].

Alternatively, we can use the new 802 ± 10 Ma Xiaofeng dykes pole from South China, the 814 ± 34 Ma Harohalli dykes pole from India [19], the ca. 820 Ma Wooltana Volcanics pole from Australia [20] and the ca. 810–795 Ma Gagwe lavas pole from the Congo craton [21,22] to reconstruct a ca. 800 Ma Rodinia similar to that of Li et al. [23] (Fig. 4a). With such use of a single set of coeval poles for reconstruction, relative paleolongitudes are non-unique, and the continental blocks can thus be moved along the paleolatitudinal small circles to make alternative reconstructions. Continents shown in gray are those without paleomagnetic constraints, and sources of their relative positions are given in the figure caption. Although the poorly constrained Laurentian ca. 800 Ma poles from the Grenville Belt and Mackenzie Mountains [12] do not fit with such a reconstruction, these are regarded as unreliable by Pisarevsky et al. [24]. Major implications of this reconstruction are that (1) Rodinia stretches from the pole to the equator at ca. 800 Ma, and (2) the supercontinent would have broken apart by ca. 750 Ma [25], with all the continental blocks distributed at low to intermediate paleolatitude (Fig. 4b).

A third possible interpretation (Fig. 5) involves

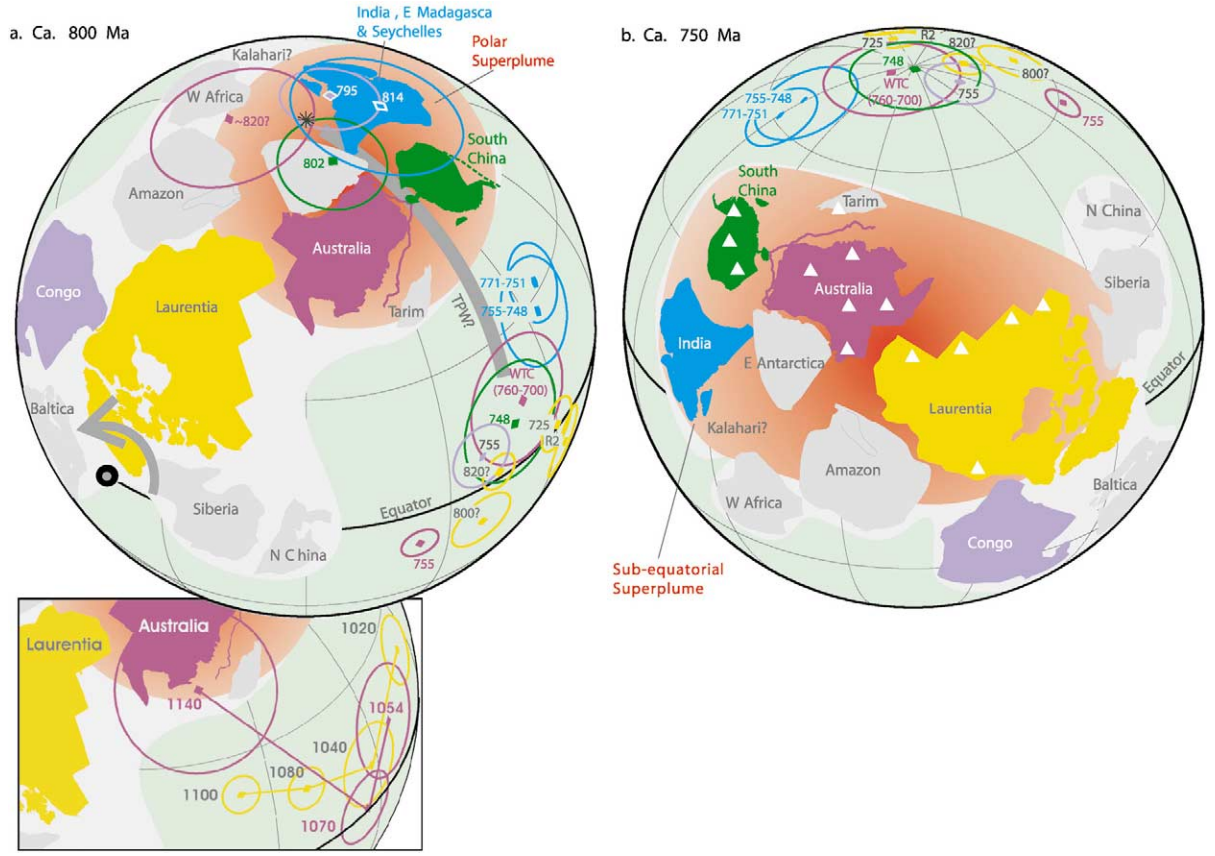

Fig. 5. Paleogeographic reconstructions of Rodinia (a) at ca. 800 Ma and (b) at ca. 750 Ma according to an alternative scenario featuring a phase of TPW between 800 and 750 Ma, and Rodinia still largely intact at ca. 750 Ma. Paleopoles are as in Fig. 4. Key Euler poles used in (a) are: Congo (45.0, 044.6, 113.4), Laurentia (33.7, −156.2, 116.2), Australia (−12.5, −013.2, 152.4), South China (32.9, 018.8, 88.3), India (20.5, 167.3, −78.3). White triangles in (b) show the occurrences of the Sturtian glacial deposits.

reconstructing Rodinia through matching the paired ca. 820–800 and 750–700 Ma paleopoles where available, rather than using paleopoles of a single age only. Again continents with no paleomagnetic data are shown in gray, but the continents constrained by paleomagnetic data are fixed relative to each other by the paired poles. There are a few salient features in the distribution of the paleopoles in this interpretation. (1) All the poles, including those from Laurentia, fall along a great circle centered around Greenland. (2) All the ca. 820–800 Ma poles, except those from Laurentia which are not regarded as reliable [24], overlap each other. (3) The three poles related to the first Neoproterozoic glacial deposits all fall close to each other: that of the Rapitan glacial deposits in western Laurentia (pole R2 [26] in Fig. 5), that of the cap dolomite above the Walsh Tillite in northwestern Australia (pole WTC [27]), and that of the Liantuo Formation in South China, which underlies and shares the same remanent direction as the Nantuo glacial deposits [14,15]. (4) The group of well-dated ca. 770–745 Ma poles, whilst clustering in a girdle distribution, cannot be matched as closely as the 820–800 Ma poles in this configuration. (5) The ca. 1100–1050 Ma poles between Laurentia and Australia also match reasonably well (see insert in Fig. 5a). The position of South China in this configuration is different from that in Fig. 4a, but it is still adjacent to

both Australia and India and thus can account for their comparable Neoproterozoic tectonostratigraphic records [4,23,28].

The combined 800–750 Ma apparent polar wander path implies pole-to-equator velocities of ca. 20 cm/yr for India and South China. Coeval data from Australia and Congo also indicate similar amounts of rapid rotations during that time interval, although their latitudinal drift rates were not as dramatic as for India and South China because of their closer affinity to the common Euler pole near Greenland. If Rodinia contained all the continents on Earth as many have argued [1–3], this would imply a rapid and wholesale 90° rotation of the entire continental land mass around an equatorial axis, motion that is most easily explained by inertial interchange TPW (IITPW [29,30]). In this interpretation, the girdle distribution of the 770–745 Ma poles is primarily due to TPW, but it could also be partly due to subordinate relative plate motions during the breakup of Rodinia.

The relative timing relationships between the formation of the supercontinent Rodinia ($\geq$900 Ma [1–3,31]), the Rodinian superplume (ca. ?860–740 Ma [4]), the possible TPW event (800–750 Ma, this study), the breakup of Rodinia (ca. 750 Ma [25] and this study), and the low-latitude glaciation at ca. 750–720 Ma [5] are intriguing. We discuss below possible genetic linkages between these events, and illustrate the sequence of events in Fig. 6.

4.2. Supercontinent–superplume coupling

As for the case of the Phanerozoic supercontinent Pangea and related superplume (superswell) event [32–34], formation of the Rodinia supercontinent by the early Neoproterozoic led to the subsequent formation of the Rodinian superplume by ca. 830 Ma [4]. This could be due partly to the thermal insulation effect of the supercontinent [32,33], and partly to the upwelling effect on the hot lower mantle by avalanched cold lithosphere [35,36] around the supercontinent. The individual plumes related to the superplume event were probably mostly 'secondary' plumes coming from the top of the superplume dome, with perhaps some 'primary' plumes coming from the lowermost mantle boundary layer (the D′) [37].

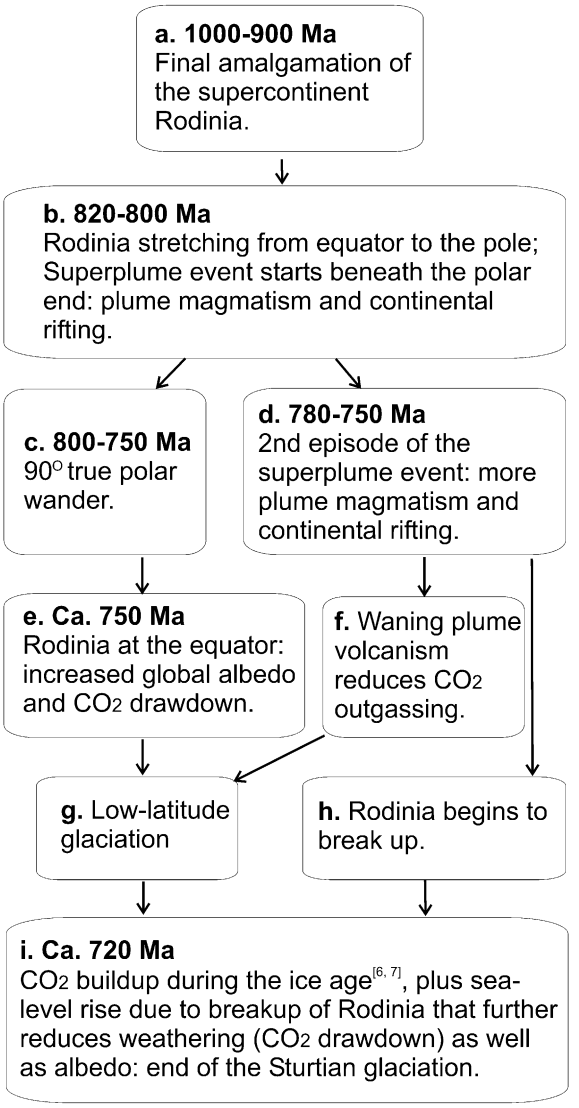

Fig. 6. A schematic flow chart illustrating the causal relationships between the major global events during early Neoproterozoic.

Such a supercontinent–superplume coupling corresponds to the supercontinent mantle upwelling segment of the super-event cycle proposed by Condie [38,39], but not to his suggested plume bombardment prior to the supercontinent formation

4.3. Superplume event as the cause for TPW

Li et al. [4] identified two episodes of major plume activities in Rodinia. The first was between 830 and 795 Ma, and it was prominent in South China, India, Australia and southern Africa but with little activity in Laurentia. The second episode (780–745 Ma) extended into much of Rodinia (Figs. 4, 5). The first episode of plume breakout, at the polar end of Rodinia, should have been associated with major perturbations to mantle mass anomalies and hence, the Earth's inertial figure. Dynamic topography across major density discontinuities in the solid Earth drives large-scale mantle upwellings to the equator via TPW [40], and large and rapid TPW rotations are to be expected in the geological record [41,42], especially during times of supercontinental breakup when symmetries of mantle convection poise the planet for polar instability [43]. The paleomagnetic reconstructions in Fig. 5 are consistent with the ca. 830–795 Ma superplume being driven to the equator in this manner. By ca. 750 Ma, regardless whether Rodinia had already started to break apart (Fig. 4b) or was still coherent (Fig. 5b), all continents, along with the superplume, were at low to intermediate paleolatitudes, a state in which the maximum moment of inertia had become aligned with the Earth's rotation axis.

4.4. Causes for low-latitude glaciations (a snowball Earth?)

Numerous mechanisms have been suggested as causes for Neoproterozoic low-latitude glaciations without altering the Earth's obliquity [44]: enhanced global albedo by emerged continents dominantly along the paleoequator [6,45], enhanced silicate weathering due to low-latitude tectonism [46] along with increased organic carbon burial [47], and CO_2 drawdown due to the weathering of large basaltic provinces [48].

These processes all may have contributed to cause the Sturtian glaciation at ca. 750–720 Ma, when the fragmenting Rodinia had migrated to dominantly low latitudes (Figs. 4b, 5b). Lack of ca. 800 Ma glacial events, despite similarly widespread extensional tectonics and plume-related volcanism at that time [4,49–51], is consistent with our new paleomagnetic data and interpretation of a polar Rodinia sector (Figs. 4a, 5a), that would have made Rodinia immune to ice-inducing albedo and chemical weathering mechanisms for glaciation at that time. Only after Rodinia had rotated to become an equatorial 'ringworld', coinciding with the waning of plume volcanism that reduced the supply of CO_2 to the atmosphere, did global energy balance and geochemical cycles respond with dramatic changes in climate [45,52].

Our model can be further tested by multidisciplinary studies of the various Neoproterozoic events concerned, and particularly through obtaining more precisely-dated, high-quality paleomagnetic data, which are still sparse for the Neoproterozoic [53].

Acknowledgements

We thank Ma Daquan, Mao Xiaodong and Wu Huaichun for assisting field sampling, P.D. Kinny for assisting SHRIMP analysis, S. Adams for paleomagnetic analysis, and S. Pisarevsky for many discussions. Critical comments from R. Van der Voo, T. Torsvik and an anonymous reviewer improved the paper. This work was supported by the Australian Research Council, and NSFC grants No. 59810761886 and 40032010B. Zircon analyses were performed on the Western Australian SHRIMP II operated by a WA university–government consortium with ARC support. Figs. 4 and 5 were produced using the PLATES software of the University of Texas at Austin, and paleomagnetic data reduction was carried out using the IAPD software package developed by T.H. Torsvik, J.C. Briden and M.A. Smethurst. This is Tectonics Special Research Center publication No. 271, and a contribution to IGCP Project 440.[VC]

References

[1] E.M. Moores, Southwest U.S.–East Antarctic (SWEAT) connection: a hypothesis, Geology 19 (1991) 425–428.
[2] I.W.D. Dalziel, Pacific margins of Laurentia and East

Antarctica – Australia as a conjugate rift pair: Evidence and implications for an Eocambrian supercontinent, Geology 19 (1991) 598–601.
[3] P.F. Hoffman, Did the breakout of Laurentia turn Gondwanaland inside-out?, Science 252 (1991) 1409–1412.
[4] Z.X. Li, X.H. Li, P.D. Kinny, J. Wang, S. Zhang, H. Zhou, Geochronology of Neoproterozoic syn-rift magmatism in the Yangtze Craton, South China and correlations with other continents: evidence for a mantle superplume that broke up Rodinia, Precambrian Res. 122 (2003) 85–109.
[5] D.A.D. Evans, Stratigraphic, geochronological, and paleomagnetic constraints upon the Neoproterozoic climatic paradox, Am. J. Sci. 300 (2000) 347–433.
[6] J.L. Kirschvink, Late Proterozoic low-latitude global glaciation: the snowball earth, in: J.W. Schopf, C. Klein (Eds.), The Proterozoic Biosphere, Cambridge University Press, Cambridge, 1992, pp. 51–52.
[7] P.F. Hoffman, A.J. Kaufman, G.P. Halverson, D.P. Schrag, A Neoproterozoic snowball earth, Science 281 (1998) 1342–1346.
[8] G. Ma, Z. Zhang, H. Li, P. Chen, Z. Huang, A geochronostratigraphical study of the Sinian System in Yangtze Platform, Bull. Yichang Inst. Geol. Miner. Res. 14 (1989) 83–124.
[9] D. Ma, Z. Xiao, The Pre-Sinian Systems, In: X. Wang, B.D. Erdtmann, X. Mao (Eds.), T106/T340: Geology of the Yangtze Gorges Area, 30th International Geological Congress Field Trip Guide, Geological Publishing House, Beijing, 1996, pp. 14–19.
[10] G. Ma, H. Lee, Z. Zhang, An investigation of the age limits of the Sinian System in South China, Bull. Yichang Inst. Geol. Miner. Res. 8 (1984) 1–29.
[11] D.R. Nelson, Compilation of SHRIMP U-Pb Zircon Geochronology Data, 1996, Geological Survey of Western Australia Record 1997/2, 1997, 189 pp.
[12] M.W. McElhinny, P.L. MacFadden, Paleomagnetism: Continents and Oceans, Academic Press, San Diego, CA, 2000, 386 pp.
[13] J.L. Kirschvink, The least-squares line and plane and the analysis of palaeomagnetic data, Geophys. J. R. Astron. Soc. 62 (1980) 699–718.
[14] D.A.D. Evans, Z.X. Li, J.L. Kirschvink, M.T.D. Wingate, A high-quality mid-Neoproterozoic paleomagnetic pole from South China, with implications for ice ages, regional stratigraphy, and the breakup configuration of Rodinia, Precambrian Res. 100 (2000) 313–334.
[15] Q.R. Zhang, J.D.A. Piper, Palaeomagnetic study of Neoproterozoic glacial rocks of the Yangzi Block: palaeolatitude and configuration of South China in the late Proterozoic Supercontinent, Precambrian Res. 85 (1997) 173–199.
[16] S.A. Pisarevsky, Z.X. Li, K. Grey, M.K. Stevens, A palaeomagnetic study of Empress 1A, a stratigraphic drillhole in the Officer Basin: evidence for a low-latitude position of Australia in the Neoproterozoic, Precambrian Res. 110 (2001) 93–108.
[17] C.M. Powell, S.A. Pisarevsky, Late neoproterozoic assembly of East Gondwana, Geology 30 (2002) 3–6.
[18] J. Wang, Z.X. Li, History of Neoproterozoic rift basins in South China: implications for Rodinia break-up, Precambrian Res. 122 (2003) 141–158.
[19] T. Radhakrishna, J. Mathew, Late Precambrian (850–800 Ma) palaeomagnetic pole for the south Indian shield from the Harohalli alkaline dykes: geotectonic implications for Gondwana reconstructions, Precambrian Res. 80 (1996) 77–87.
[20] M.O. McWilliams, M.W. McElhinny, Late Precambrian paleomagnetism of Australia: the Adelaide Geosyncline, J. Geol. 88 (1980) 1–26.
[21] J.G. Meert, R. Van der Voo, S. Ayub, Paleomagnetic investigation of the Neoproterozoic Gagwe lavas and Mbozi Complex, Tanzania and the assembly of Gondwana, Precambrian Res. 74 (1995) 225–244.
[22] A. Deblond, L.E. Punzalan, A. Boven, L. Tack, The Malagarazi Supergroup of southeast Burundi and its correlative Bukoba Supergroup of northwest Tanzania: Neo- and Mesoproterozoic chronostratigraphic constraints from Ar–Ar ages on mafic intrusive rocks, J. Afr. Earth Sci. 32 (2001) 435–449.
[23] Z.X. Li, X.H. Li, P.D. Kinny, J. Wang, The breakup of Rodinia: did it start with a mantle plume beneath South China?, Earth Planet. Sci. Lett. 173 (1999) 171–181.
[24] S.A. Pisarevsky, M.T.D. Wingate, C.M. Powell, S. Johnson, D.A.D. Evans, Models of Rodinia assembly and fragmentation, in: M. Yoshida, B.F. Windley, S. Dasgupta (Eds.), Proterozoic East Gondwana: Supercontinent Assembly and Breakup, Geol. Soc. London Spec. Publ. 206, 2003, pp. 35–55.
[25] M.T.D. Wingate, J.W. Giddings, Age and palaeomagnetism of the Mundine Well dyke swarm, Western Australia: implications for an Australia–Laurentia connection at 755 Ma, Precambrian Res. 100 (2000) 335–357.
[26] J.K. Park, Paleomagnetic evidence for low-latitude glaciation during deposition of the Neoproterozoic Rapitan Group, Mackenzie Mountains, N.W.T., Canada, Can. J. Earth Sci. 34 (1997) 34–49.
[27] Z.X. Li, New palaeomagnetic results from the 'cap dolomite' of the Neoproterozoic Walsh Tillite, northwestern Australia, Precambrian Res. 100 (2000) 359–370.
[28] G. Jiang, L.E. Sohl, N. Christie-Blick, Neoproterozoic stratigraphic comparison of the Lesser Himalaya (India) and Yangtze block (South China): Paleogeographic implications, Geology 31 (2003) 917–920.
[29] J.L. Kirschvink, R.L. Ripperdan, D.A. Evans, Evidence for a large-scale reorganization of Early Cambrian continental masses by inertial interchange true polar wander, Science 277 (1997) 541–545.
[30] D.A. Evans, True polar wander, a supercontinental legacy, Earth Planet. Sci. Lett. 157 (1998) 1–8.
[31] Z.X. Li, M. Cho, X.H. Li, Precambrian tectonics of East Asia and relevance to supercontinent evolution, Precambrian Res. 122 (2003) 1–6.

[32] D.L. Anderson, Hotspots, polar wander, Mesozoic convection and the geoid, Nature 297 (1982) 391–393.
[33] D.L. Anderson, Superplume or supercontinents?, Geology 22 (1994) 39–42.
[34] M. Doblas, R. Oyarzun, R.J. Lopez, J.M. Cebria, N. Youbi, V. Mahecha, M. Lago, A. Pocovi, B. Cabanis, Permo-Carboniferous volcanism in Europe and Northwest Africa: a superplume exhaust valve in the centre of Pangaea?, J. Afr. Earth Sci. 26 (1998) 89–99.
[35] L.H. Kellogg, B.H. Hager, R.D. Van der Hilst, Compositional stratification in the deep mantle, Science 283 (1999) 1881–1884.
[36] E.M. Moores, L.H. Kellogg, Y. Dilek, Tethyan ophiolites, mantle convection, and tectonic 'historical contingency': A resolution of the 'ophiolite conundrum', in: Y. Dilek, E.M. Moores, D. Elthon, A. Nicolas (Eds.), Ophiolites and Oceanic Crust: New Insights from Field Studies and the Ocean Drilling Program, Geological Society of America, Boulder, CO, GSA Special Paper 349, 2000, pp. 3–12.
[37] V. Courtillot, A. Davaille, J. Besse, J. Stock, Three distinct types of hotspots in the Earth's mantle, Earth Planet. Sci. Lett. 205 (2003) 295–308.
[38] K.C. Condie, Episodic continental growth and supercontinents: a mantle avalanche connection?, Earth Planet. Sci. Lett. 163 (1998) 97–108.
[39] K.C. Condie, Episodic continental growth models: afterthoughts and extensions, Tectonophysics 322 (2000) 153–162.
[40] B.H. Hager, R.W. Clayton, M.A. Richards, A.M. Comer, A.M. Dziewonski, Lower mantle heterogeneity, dynamic topography and the geoid, Nature 313 (1985) 541–545.
[41] M.A. Richards, H.P. Bunge, Y. Ricard, J.R. Baumgardner, Polar wandering in mantle convection models, Geophys. Res. Lett. 26 (1999) 1777–1780.
[42] R. Van der Voo, True polar wander during the middle Paleozoic?, Earth Planet. Sci. Lett. 122 (1994) 239–243.
[43] D.A.D. Evans, True polar wander and supercontinents, Tectonophysics 362 (2003) 303–320.
[44] G.E. Williams, Late Precambrian glacial climate and the Earth's obliquity, Geol. Mag. 112 (1975) 441–465.
[45] T.R. Worsley, D.L. Kidder, First-order coupling of paleogeography and CO_2, with global surface temperature and its latitudinal contrast, Geology 19 (1991) 1161–1164.
[46] G.M. Young, The geological record of glaciation: Relevance to the climatic history of the Earth, Geosci. Can. 18 (1991) 100–108.
[47] D.P. Schrag, R.A. Berner, P.F. Hoffman, G.P. Halverson, On the initiation of a snowball Earth, Geochem. Geophys. Geosyst. 3 (2002) 10.1029/2001GC000219.
[48] Y. Godderis, Y. Donnadieu, A. Nédélec, B. Dupré, C. Dessert, A. Grard, G. Ramstein, L.M. Francois, The Sturtian 'snowball' glaciation: fire and ice, Earth Planet. Sci. Lett. 211 (2003) 1–12.
[49] J.X. Zhao, M.T. Malcolm, R.J. Korsch, Characterisation of a plume-related ~800 Ma magmatic event and its implications for basin formation in central-southern Australia, Earth Planet. Sci. Lett. 121 (1994) 349–367.
[50] H.E. Frimmel, R.E. Zartman, A. Spath, The Richtersveld Igneous Complex, South Africa: U–Pb zircon and geochemical evidence for the beginning of Neoproterozoic continental breakup, J. Geol. 109 (2001) 493–508.
[51] Z.X. Li, X.H. Li, H.W. Zhou, P.D. Kinny, Grenvillian continental collision in south China: New SHRIMP U–Pb zircon results and implications for the configuration of Rodinia, Geology 30 (2002) 163–166.
[52] H.G. Marshall, J.C.G. Walker, W.R. Kuhn, Long-term climate change and the geochemical cycle of carbon, J. Geophys. Res. 93 (1988) 791–801.
[53] T.H. Torsvik, The Rodinia jigsaw puzzle, Science 300 (2003) 1379–1381.
[54] T.H. Torsvik, L.M. Carter, L.D. Ashwal, S.K. Bhushan, M.K. Pandit, B. Jamtveit, Rodinia refined or obscured: palaeomagnetism of the Malani Igneous Suite (NW India), Precambrian Res. 108 (2001) 319–333.
[55] T.H. Torsvik, L.D. Ashwal, R.D. Tucker, E.A. Eide, Neoproterozoic geochronology and palaeogeography of the Seychelles microcontinent: the India link, Precambrian Res. 110 (2001) 47–59.
[56] Z.X. Li, New palaeomagnetic results from the 'cap dolomite' of the Neoproterozoic Walsh Tillite, northwestern Australia, Precambrian Res. 100 (2000) 359–370.
[57] B.R. Frost, O.V. Avchenko, K.R. Chamberlain, C.D. Frost, Evidence for extensive Proterozoic remobilization of the Aldan shield and implications for Proterozoic plate tectonic reconstructions of Siberia and Laurentia, Precambrian Res. 89 (1998) 1–23.
[58] Z.X. Li, L. Zhang, C.M. Powell, Positions of the East Asian cratons in the Neoproterozoic supercontinent Rodinia, Aust. J. Earth Sci. 43 (1996) 593–604.
[59] E. Tohver, B. Van der Pluijm, R. Van der Voo, G. Rizzotto, J.E. Scandolara, Paleogeography of the Amazon Craton at 1.2 Ga: early Grenvillian collision with the Llano segment of Laurentia, Earth Planet. Sci. Lett. 199 (2002) 185–200.